Automated Synthesis of Metasurface Antennas

Automated Synthesis of Metasurface Antennas

Marcello Zucchi*, Francesco Vernì*, Marco Righero†, Giuseppe Vecchi*
*Department of Electronics and Telecommunications, Politecnico di Torino, Turin, Italy, marcello.zucchi@polito.it
†Advanced Computing and Applications, Fondazione LINKS, Turin, Italy

***Abstract*—This paper proposes an algorithm for the automated design of metasurface antennas. From the knowledge of an objective radiation field and of an incident field, it allows to synthesize the required surface impedance on the radiating aperture. A scalar impedance boundary condition is employed in the integral equation formulation of the electromagnetic problem. The approach is entirely numerical, based on an iterative algorithm able to enforce both physical and feasibility constraints. This procedure was applied to the design of a leaky-wave antenna at 30 GHz and a circular metasurface antenna at 17 GHz. The results showed a good performance compared to a reference analytical design.**

***Index Terms*—antenna optimization, metasurface antennas, method of moments (MoM), impedance boundary condition (IBC).**

I. Introduction

Metasurface antennas (MTS) represent one of the most promising technology for the realization of low-profile antennas, due to their low losses and ease of manufacturing [1]. They are characterized by a surface impedance distribution, which is modulated to produce the desired radiation properties.

The design of this class of antennas is challenging due to their multi-scale features, with the large electrical size of the radiating aperture combined with the fine details of the patterning. For this reason, a direct optimization is often unfeasible from the computational point of view, and the process is usually divided in two steps: 1) design of a continuous impedance profile that yields the required radiation performance (in terms of gain and polarization), and 2) implementation of the resulting profile by means of a properly textured metallic layout (printed on a dielectric substrate). Our approach addresses the first step, while the second one is typically carried out with well-known procedures [2].

In the literature, different methods have been proposed for the design of these antennas. In [3], the authors employed an analytical local approximation for the design of spiral leaky-wave antennas. More recently, a numerical approach [4], [5] has been introduced for the synthesis of circular metasurface antennas, with a full wave solution based on entire-domain basis functions. In [6], [7] a related numerical inversion methodology has been applied to the design of metasurface screens, with explicit enforcement of power conservation. All these methods focus on the synthesis of the impedance profile. However, they rely on a number of assumptions (circular geometry, sinusoidal modulation, predefined average impedance value, etc.) that limit their applicability.

The present paper presents an alternative approach that is entirely numerical and can be applied to metasurfaces with general configurations. It is based on an iterative algorithm and is able to include physical constraints (power conservation) as well as feasibility requirements (local reactivity). It relies on a surface integral equation for the numerical solution of the associated electromagnetic problem with the Method of Moments (MoM).

II. Synthesis of Metasurface Antennas

A. Impedance Boundary Condition

The metasurface antenna is modeled by means of an infinitely thin layer of penetrable surface impedance on top of a dielectric grounded substrate. This surface is assumed to have an isotropic electric response represented by a scalar Impedance Boundary Condition (IBC), which relates the tangential electric field to the jump of the tangential magnetic field across the impedance layer:

$$\boldsymbol{E}_{\mathrm{t}} = Z_{\mathrm{s}}\, \hat{\boldsymbol{n}} \times \left(\boldsymbol{H}^{+} - \boldsymbol{H}^{-} \right) = Z_{\mathrm{s}}\, \boldsymbol{J}_{\mathrm{s}}, \tag{1}$$

where $\boldsymbol{J}_{\mathrm{s}}$ is the equivalent surface electric current. This formulation leads to a stable numerical treatment in terms of an Electric Field Integral Equation (EFIE-IBC) solved with the Method of Moments, as demonstrated in [8].

In the case of a scalar IBC, the requirement for local reactivity (no gain, no losses) forces the impedance to be purely imaginary locally on the surface.

B. Numerical Algorithm

The algorithm requires the discretization of the radiating surface with a triangular mesh. The equivalent current is then expanded by means of Rao-Wilton-Glisson (RWG) basis functions, while the surface impedance is assumed constant on each triangular patch (pulse basis expansion).

The preliminary phase is completed by the computation and storage of the MoM system matrix. The combined effect of the dielectric substrate and of the ground plane is taken into account inside the Green's function employed in the MoM solution.

The complete algorithm can be summarized in the following steps:

1) From the knowledge of the objective field, an equivalent surface current is obtained through a source inversion; this inversion is carried out by means of a least square minimum norm algorithm and provides the visible part of the current spectrum.
2) Given this current, the source amplitude and phase are optimized to minimize local losses (ensuring power conservation).

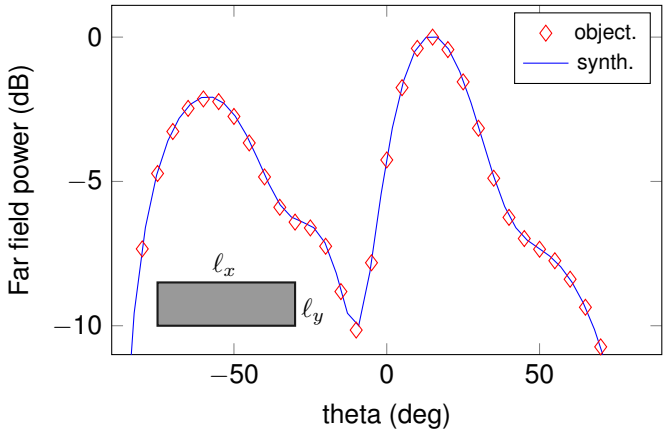

Fig. 1: Far field power pattern of the resulting leaky-wave antenna ($\phi = 0°$ plane cut): synthesized far field (solid line) and samples of the objective field used in the synthesis process (markers).

3) The surface impedance is computed over each triangular patch by testing both sides of (1) with a given set of local weighting functions and solving the resulting system.
4) Reactivity is enforced by setting to zero the residual real part of the local impedance.
5) With this new impedance profile, a new EFIE-IBC system is solved, and the resulting current is compared to the previous one: if the difference is within the prescribed tolerance the algorithm stops, otherwise it continues.
6) The resulting surface current is modified in order to radiate the objective far field. This correction is determined by inverting the difference between the field radiated by the current and the objective one. Next, these steps are repeated from step 2 until convergence is reached.

At the end of this process, a specific impedance profile is provided. This profile is piecewise constant, as dictated by the discretization, and can be readily implemented.

With regard to the computational effort, the procedure is based on a number of calculations that are suitable to numerical acceleration. In particular, the far field computation and the EFIE-IBC solution are the most computationally intensive steps and both of them can be accelerated through FFT-based, well-known algorithms. Together with the impedance reconstruction (step 3), which has a linear complexity, the resulting overall asymptotic complexity is $O(N \log N)$.

III. Results

A. Leaky-wave Antenna

To verify its effectiveness, the algorithm has been applied to the synthesis of a planar leaky-wave antenna. The antenna is composed of a rectangular impedance surface of width $\ell_x = 18.0\,\mathrm{mm}$ and height $\ell_y = 5.0\,\mathrm{mm}$, printed on a grounded dielectric slab with $\varepsilon_\mathrm{r} = 3.0$ and thickness $h = 0.762\,\mathrm{mm}$. As is usually the case for metasurface antennas, the incident field is represented by a cylindrical TM surface wave, with

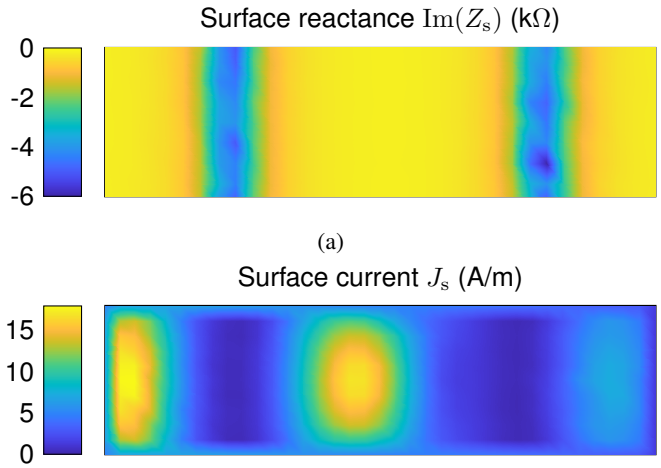

Fig. 2: Synthesized leaky-wave antenna: (a) reactance (imaginary part) of the surface impedance, (b) surface current excited by the incident electric field.

the phase center at $x_\mathrm{feed} = -(\ell_x + \ell_y)/2$. For the numerical solution, the surface was discretized with a mesh of size $\approx \lambda/20$. No numerical acceleration was employed due to the limited size of the considered problem.

The objective far field was obtained from the analytical approximated design of a sinusoidally modulated leaky-wave antenna [9], with a broadside radiation pattern at the frequency $f = 30\,\mathrm{GHz}$. It was sampled on a uniform grid of $N_\theta \times N_\phi$ spherical points (θ, ϕ) spanning the upper half sphere, with $N_\theta = 37$ and $N_\phi = 10$.

The resulting far field power pattern is shown in Fig. 1. As is evident, there's a fairly good agreement between the objective and the synthesized fields. Looking at the corresponding surface impedance (Fig. 2a) and current (Fig. 2b), their pro-

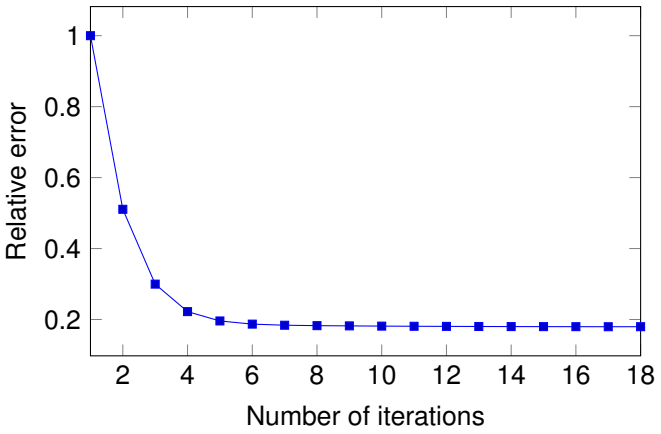

Fig. 3: Convergence of the iterative synthesis algorithm for the leaky-wave antenna. The relative error is computed as the difference of the current before and after the solution of the EFIE-IBC (step 5).

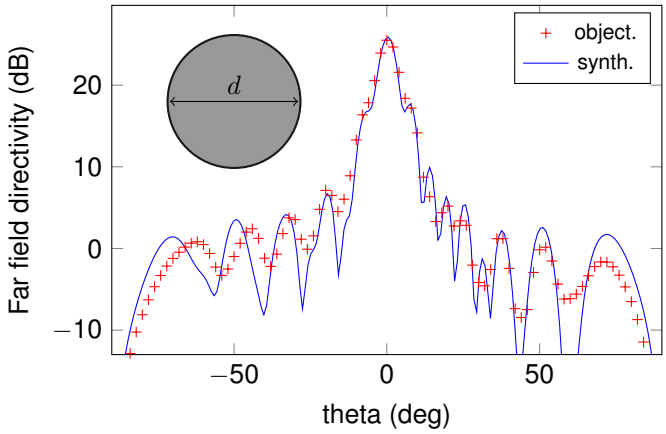

Fig. 4: Far field directivity pattern of the resulting circular metasurface antenna ($\phi = 0°$ plane cut): synthesized far field (solid line) and samples of the objective field used in the synthesis process (markers).

file follow closely that of the analytical solution. Although not required by the algorithm, this consistency validates the proposed approach. The real part of the impedance is null everywhere on the surface, as expected from the enforcement of reactivity. Finally, the optimization took a total of 18 iterations to converge (Fig. 3).

B. Circular Metasurface Antenna

To further assess its validity, the algorithm has then been applied to the design of an electrically large metasurface antenna, at a frequency of 17 GHz. It is of circular shape, with a diameter $d = 0.2\,\mathrm{m} \approx 11\lambda$, placed on a grounded dielectric slab with $\varepsilon_\mathrm{r} = 3.66$ and thickness $h = 1.524\,\mathrm{mm}$. The incident field is a cylindrical TM surface wave, propagating radially from the center of the disk. The surface is discretized with a triangular mesh of size $\approx \lambda/10$. Given the large electrical size of the problem, the numerical solution of the integral equation has been accelerated by means of entire domain basis functions [10].

The objective far field was derived from the reference design of a sinusoidally modulated metasurface [11], characterized by a broadside beam and low sidelobe level. The sampling grid was uniform, with $N_\theta = 45$ and $N_\phi = 90$.

The directivity pattern is shown in Fig. 4: the agreement between the objective and synthesized far field is satisfactory. The reconstructed impedance profile (Fig. 5a) and surface current (Fig. 5b) show the expected spiral behaviour, typical of a sinusoidally modulated metasurface antenna.

IV. Conclusion

A novel algorithm for the automated design of metasurface antennas has been presented. From the knowledge of the objective far field and the incident electric field, it allows the synthesis of a practically realizable impedance profile. It is capable of enforcing power conservation and feasibility constraints, without a priori assumption on the impedance

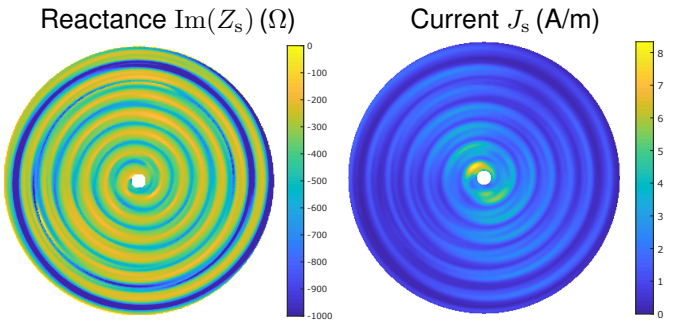

(a) (b)

Fig. 5: Synthesized circular metasurface antenna: (a) reactance (imaginary part) of the surface impedance, (b) surface current excited by the incident electric field.

distribution. The algorithm was tested by designing a planar leaky-wave antenna and a circular metasurface antenna. In both cases, satisfactory results were obtained, supporting the effectiveness of the proposed approach.

Acknowledgment

This work was supported by the Italian Ministry of Research PRIN 2017S29ZLA “Metasurface Antennas for Space Applications”.

References

[1] M. Faenzi, G. Minatti, D. González-Ovejero, F. Caminita, E. Martini, C. D. Giovampaola, and S. Maci, “Metasurface Antennas: New Models, Applications and Realizations,” *Scientific Reports*, vol. 9, no. 1, pp. 1–14, Jul. 2019. [Online]. Available: https://www.nature.com/articles/s41598-019-46522-z

[2] A. M. Patel and A. Grbic, “Effective Surface Impedance of a Printed-Circuit Tensor Impedance Surface (PCTIS),” *IEEE Transactions on Microwave Theory and Techniques*, vol. 61, no. 4, pp. 1403–1413, Apr. 2013.

[3] G. Minatti, F. Caminita, E. Martini, M. Sabbadini, and S. Maci, “Synthesis of Modulated-Metasurface Antennas With Amplitude, Phase, and Polarization Control,” *IEEE Transactions on Antennas and Propagation*, vol. 64, no. 9, pp. 3907–3919, Sep. 2016.

[4] M. Bodehou, C. Craeye, and I. Huynen, “Electric Field Integral Equation-Based Synthesis of Elliptical-Domain Metasurface Antennas,” *IEEE Transactions on Antennas and Propagation*, vol. 67, no. 2, pp. 1270–1274, Feb. 2019.

[5] M. Bodehou, C. Craeye, E. Martini, and I. Huynen, “A Quasi-Direct Method for the Surface Impedance Design of Modulated Metasurface Antennas,” *IEEE Transactions on Antennas and Propagation*, vol. 67, no. 1, pp. 24–36, Jan. 2019.

[6] T. Brown, C. Narendra, Y. Vahabzadeh, C. Caloz, and P. Mojabi, “On the Use of Electromagnetic Inversion for Metasurface Design,” *IEEE Transactions on Antennas and Propagation*, vol. 68, no. 3, pp. 1812–1824, Mar. 2020.

[7] T. Brown, Y. Vahabzadeh, C. Caloz, and P. Mojabi, “Electromagnetic Inversion With Local Power Conservation for Metasurface Design,” *IEEE Antennas and Wireless Propagation Letters*, vol. 19, no. 8, pp. 1291–1295, Aug. 2020.

[8] M. A. Francavilla, E. Martini, S. Maci, and G. Vecchi, “On the Numerical Simulation of Metasurfaces With Impedance Boundary Condition Integral Equations,” *IEEE Transactions on Antennas and Propagation*, vol. 63, no. 5, pp. 2153–2161, May 2015.

[9] A. M. Patel and A. Grbic, “A Printed Leaky-Wave Antenna Based on a Sinusoidally-Modulated Reactance Surface,” *IEEE Transactions on Antennas and Propagation*, vol. 59, no. 6, pp. 2087–2096, Jun. 2011.

[10] F. Vernì, M. Righero, and G. Vecchi, "On the Use of Entire-Domain Basis Functions and Fast Factorizations for the Design of Modulated Metasurface," *IEEE Transactions on Antennas and Propagation*, vol. 68, no. 5, pp. 3824–3833, May 2020.

[11] G. Minatti, M. Faenzi, E. Martini, F. Caminita, P. De Vita, D. González-Ovejero, M. Sabbadini, and S. Maci, "Modulated Metasurface Antennas for Space: Synthesis, Analysis and Realizations," *IEEE Transactions on Antennas and Propagation*, vol. 63, no. 4, pp. 1288–1300, Apr. 2015.